Eur. Phys. J. Appl. Phys. (2014) 68: 30403
DOI: 10.1051/epjap/2014140239

THE EUROPEAN PHYSICAL JOURNAL APPLIED PHYSICS

Regular Article

A water-based molecular flip-flop

Yu Wang[1,2,a] and Jiping Huang[3,b]

[1] Department of Physics, Zhejiang Agriculture and Forestry University, Hangzhou, Linan 311300, P.R. China
[2] Zhejiang Provincial Key Laboratory of Chemical Utilization of Forestry Biomass, Zhejiang Agriculture and Forestry University, Hangzhou, Linan 311300, P.R. China
[3] Department of Physics, Fudan University, Shanghai 200433, P.R. China

Received: 5 June 2014 / Received in final form: 28 October 2014 / Accepted: 6 November 2014
Published online: 12 December 2014 –

Abstract. The flip-flop, which has been widely used in digital circuits, has two stable states and can be used to store state information. Because traditional flip-flops based on digital circuits suffer from a barrier to higher performance, it is necessary to explore some new alternative devices. For this purpose, we utilize molecular dynamics simulations to design a molecular flip-flop, which contains one water molecule confined within a single-walled carbon nanotube. Its two states can be switched within 0.5 ps (2000 GHz), and its state information can be exported by the charged atomic-force microscope force probes. The mechanism of the flip-flop depends on the behavior of a water molecule in a nonuniform electric field. In particular, a water molecule always moves toward the location of lowest electric energy in a nonuniform electric field generated by point charges. The resulting flip-flop could be utilized for designing nanoscale devices.

1 Introduction

In digital electronics, a flip-flop [1] is a basic circuit that can store state information using states 0 and 1. The states can be changed from 0 to 1 (or from 1 to 0) by one or more input signals, and the new state information can be immediately exported. The flip-flop unit plays an important role in traditional electronic computers, which are based on silicon materials. However, traditional electronic computers will soon face severe challenges in achieving higher levels of computing performance. To overcome these limitations, researchers are attempting to design new computational schemes in which microfluidic computations [2–4] have shown promise. Microfluidic computations are based on a microfluidic lab-on-a-chip [5–7] in which picoliter-level fluids can be precisely controlled and manipulated in the microchannel. The lab-on-a-chip has been experimentally used to design elementary computational units, such as microfluidic memory storage devices [2] and microfluidic logic gates [3,4]. Flip-flop devices are also particularly important for microfluidic computations.

In 2009, we theoretically proposed a flip-flop device [8] based on a microfluidic system. In the device, a lossless dielectric microparticle and lossless dielectric liquid are contained in a microchannel, and three point microelectrodes are fixed in a triangular pattern outside the microchannel. The microparticle suspended in the dielectric liquid can be polarized by an electric field. The interaction between the polarized microparticle and the nonuniform electric field generated by the microelectrodes yields a nonzero net electrostatic force acting on the microparticle. As the two microelectrodes located on the same side of the microchannel are separated, two possible stable positions are identified for the microparticle that can be defined as state 0 and state 1. When the single microelectrode on the opposite side of the microchannel emits an electric pulse with a suitable duration, the microparticle can be driven from state 0 to 1 (or from 1 to 0). Thus, the device has a flip-flop function. Nonetheless, there are two fundamental problems related to the design. First, the state switch time of the flip-flop is on the order of a microsecond, which is much slower than that of an electronic flip-flop (Problem I). Second, the export of the binary state information of the flip-flop remains unresolved (Problem II).

To overcome Problems I and II, we introduce a nanofluid-based flip-flop scheme based on the previous design [8]. The details of this scheme are shown in Figure 1. To resolve Problem I, the microchannel and the microparticle are replaced by a single-walled carbon nanotube (SWCNT) and a water molecule, respectively. There are four reasons why we selected the water molecule and SWCNT. First, water is abundant on earth. Second, a water molecule is neutral as a whole but has a strong dipole moment [9]; thus, the interaction between the nonuniform electric field and the water molecule can yield a nonzero net electrostatic force on the water molecule. Third, a water molecule acted on by a nonzero force will

[a] e-mail: yuwang_zafu@126.com
[b] e-mail: jphuang@fudan.edu.cn

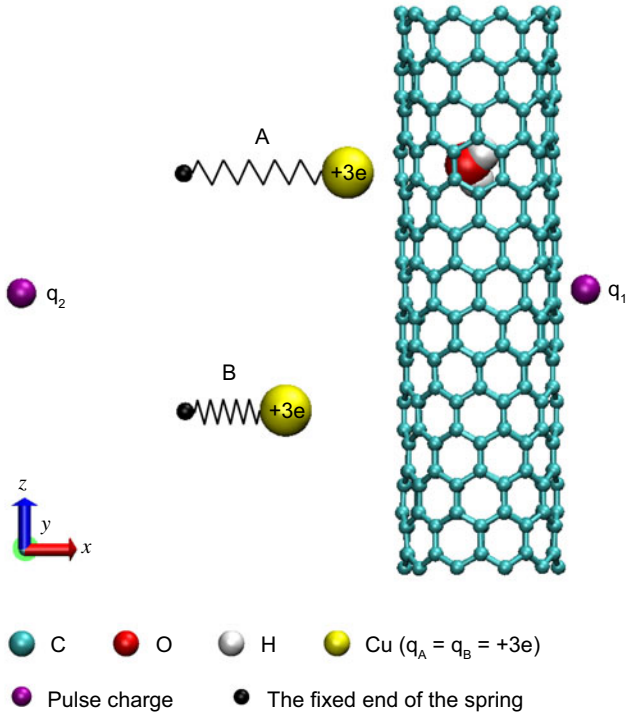

Fig. 1. Snapshot of the simulation framework. The designed flip-flop consists of three components: input, conversion and output. The input component consists of pulse charges q_1 and q_2. The conversion component contains water molecules in a zigzag $(10, 0)$ single-walled carbon nanotube with diameter $d = 0.772\,\text{nm}$. The output component has two ideal springs (A and B), which equally displace two copper-based atomic-force microscope force probes for reducing the calculational load. There is a constant charge with a value of $+3e$ on each copper atom ($q_A = q_B = +3e$).

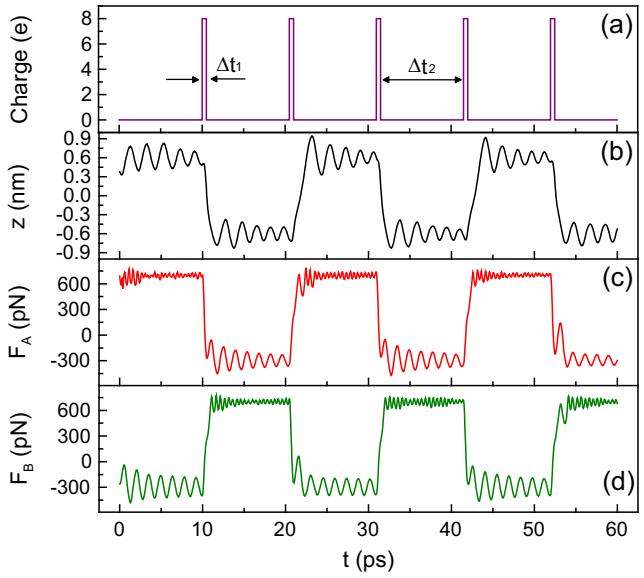

Fig. 2. (a) The charge signal for a pulse charge, q_1 or q_2, is plotted with respect to time, t. Here, the width is $\triangle t_1 = 0.5\,\text{ps}$, and the interval is $\triangle t_2 = 10\,\text{ps}$. (b) The z-directed position of the water molecule. (c) The force F_A measured by Spring A, and (d) the force F_B measured by Spring B.

rapidly respond because the water molecule has a very small mass. Finally, as a result of the low adhesion of the SWCNT surface, a water molecule located in a SWCNT with a sufficient diameter can move smoothly along one dimension [10]. To resolve Problem II, we utilize two charged atomic-force microscope (AFM) probes [11–13] to detect the state information of the water molecule.

2 Model details and molecular dynamics simulations

In this work, we utilize molecular dynamics simulations, which have been widely used to investigate systems of carbon nanotubes and water molecules [10,14–22]. Our simulation framework is shown in Figure 1. The flip-flop consists of three components: input, conversion and output components. The input component contains charges q_1 and q_2, which can both emit a periodic electric pulse. In the simulations, q_1 is located at the coordinate origin, while q_2 is fixed at coordinate $(-2.844\,\text{nm}, 0.000\,\text{nm}, 0.000\,\text{nm})$. The conversion component contains a water molecule in a zigzag $(10, 0)$ SWCNT with diameter $d = 0.772\,\text{nm}$. To keep the SWCNT in a fixed position, carbon atoms at each end of the SWCNT are constrained [19]. In fact, carbon nanotubes can connect with other molecules through covalent bonds [16,23,24]; hence, it is possible to fix the SWCNT position in experiments. A water molecule restrained in a fixed SWCNT can only move along the SWCNT axial direction (or the z-direction as shown in Fig. 1) [19]. The charges q_1 and q_2 are placed $0.150\,\text{nm}$ and $1.922\,\text{nm}$ from the surface of the SWCNT, respectively. The output component consists of two copper-based AFM force probes. To reduce the computational work, in this work, each AFM probe is replaced by an equivalent ideal spring, and only the copper atom at the apex of each force probe is retained. This force probe simplification has been widely used to investigate the mechanical properties of nanoscale systems [25–28]. Moreover, in this work, the fixed end of the spring A and B is set at coordinates $(-2.022\,\text{nm}, 0.000\,\text{nm}, 0.600\,\text{nm})$ and $(-2.022\,\text{nm}, 0.000\,\text{nm}, -0.600\,\text{nm})$, respectively. The force in the spring is given by Hooke's law, $F = k(l - l_0)$, with stiffness $k = 3320\,\text{pN/nm}$. Here, l denotes the distance between the free end (or the copper atom) and fixed end of the spring, and $l_0 = 0.600\,\text{nm}$ is a constant representing the length of the spring at equilibrium. For convenience, the charge distributions of the input and output components are also simplified in the simulations. Each copper atom has a charge with a constant value of $+3e$ ($q_A = q_B = +3e$, where e is the elementary charge, $e = 1.6 \times 10^{-19}\,\text{C}$). Furthermore, both q_1 and q_2 have a pulse charge with a peak value of $+8e$ (see Fig. 2a). The charges q_1, q_2, q_A and q_B are regarded as ideal point charges, namely, their volumes are small enough to be neglected. The electric charge quantity of q_A or q_B is concentrated on each copper atom. The point charges are used

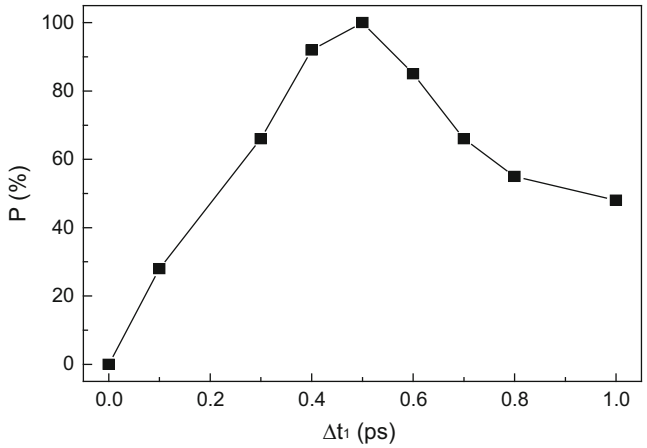

Fig. 3. Success rate P of the state shift as a function of $\triangle t_1$ for 1000 pulses of $q_1 = q_2 = +8e$ with $\triangle t_2$= 10 ps.

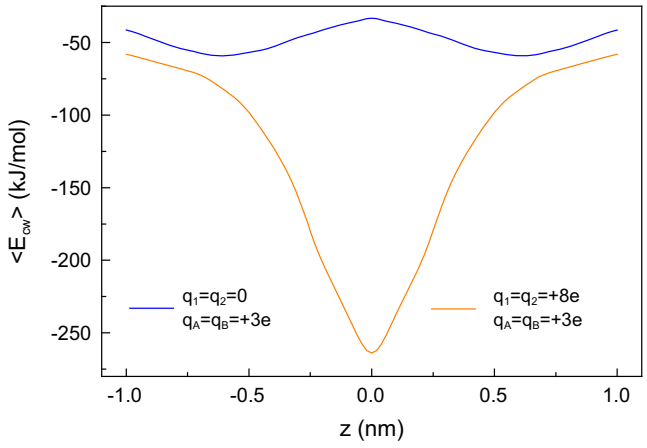

Fig. 4. Mean electrostatic interaction energy $\langle E_{cw} \rangle$ between the water molecule and charges as a function of z.

to generate a nonuniform electric field acting on the water molecule, which can be equivalently realized by adjusting real charge distributions on nanoelectrodes and charged AFM probes according to the superposition principle of electrical fields. The charges q_1 and q_2 are given different tasks in our design. In particular, because the carbon nanotube is closer to q_1 than q_2, the water molecule is primarily influenced by q_1. However, if only q_1 exists in the system, it will probably interfere with the force signal output of the charged copper atoms. To counteract this interference, q_2 is placed at a suitable position, where q_2 and q_1 are symmetric with respect to the two copper atoms of springs A and B at equilibrium. The emission of q_2 is precisely synchronized with that of q_1. In these systems, the screening effect of the SWCNT must be considered [15,17,18,20]. In fact, the charges we adopted could be regarded as effective charges, and realistic charge quantities should be made increased by a factor related to the screening effect [15,17,18,20].

All the simulations are performed in a canonical ensemble [29] at a constant temperature of 300 K using the molecular dynamics package, Gromacs 4.0.5 [30]. Non-periodic boundary conditions are applied in the simulations. The van der Waals potential and electrostatic potential are calculated with a long cutoff of 10.0 nm, which exceeds the maximum distance between two atoms in the current system. All SWCNT force field parameters are taken from Hummer et al. [10], while the van der Waals parameters of copper are taken from Agrawal et al. [31], and the Tip3p water model [32] is adopted where the charge quantity on the oxygen atom is −0.834 e and that on a hydrogen atom is +0.417 e. The simulation for each parameter set runs for 50 ns. A time step of 2.0 fs is used, and data are collected every 40.0 fs.

3 Results and discussion

Figure 2 shows a representative result of simulations. In this case, we choose the width $\triangle t_1 = 0.5$ ps and the interval $\triangle t_2 = 10$ ps for the q_1 and q_2 pulse signals (Fig. 2a). The water molecule in the SWCNT has two stable positions at $z = 0.614 \pm 0.020$ nm and -0.613 ± 0.019 nm (Fig. 2b), which may be defined as state 0 and state 1, respectively. Interestingly, when q_1 and q_2 simultaneously emit a charge pulse, the water molecule can immediately shift from 0 to 1 (or from 1 to 0) on the picosecond timescale. Owing to the electrostatic attraction between the water molecule and the charges (q_A and q_B), the water molecule is under state 0 or state 1. Meanwhile, spring A (or B) reaches a maximum force of $+705 \pm 12$ pN (Figs. 2c or 2d, respectively). That is, the state of the water molecule can be determined by the force signal output of springs A and B. Thus, we have realized the basic functionality of the flip-flop.

To proceed, the work efficiency of the flip-flop, which can be evaluated by the success rate of the state switch, should be identified. Here, we test the success rate of the shift by adjusting the pulse width $\triangle t_1$; see Figure 3. The success rate P reaches a peak of 100% at $\triangle t_1 = 0.5$ ps. When $\triangle t_1 < 0.5$ ps or $\triangle t_1 > 0.5$ ps, $P < 100\%$, illustrating low state shift success rates.

To understand the above phenomena, we calculate the mean electrostatic interaction energy between the water molecule and charges; see Figure 4. As q_1 and q_2 are closed ($q_1 = q_2 = 0$), symmetrical potential traps appear at opposite sides of the curve, and the system shows bistability. The water molecule will overcome a potential barrier at $z = 0$ if it is able to shift from one state to the other. Thus, the water molecule can steadily return to $z \approx 0.61$ nm (state 0) or $z \approx -0.61$ nm (state 1) with the same probability. When q_1 and q_2 are opened ($q_1 = q_2 = +8e$), a deep potential trap exists at the middle of the curve. The system shows monostability, and the water molecule moves toward $z = 0$. Thus, the state shift of the water molecule from 0 to 1 (or from 1 to 0) is caused by the alternation of bistability and monostability. Figure 3 reveals that satisfactory shifts between the two states depend on an appropriate pulse time width ($\triangle t_1 = 0.5$ ps) for q_1 and q_2. This behavior can also be explained by Figure 4. When $\triangle t_1 < 0.5$ ps, the water molecule cannot obtain enough kinetic energy from q_1 and q_2; on the

other hand, when $\triangle t_1 > 0.5\,\text{ps}$, because the water molecule remains near the monostable potential trap of $z = 0$ for a relatively long time, its kinetic energy is dissipated.

4 Conclusion and outlook

We have designed a molecular flip-flop consisting of a water molecule, a small-diameter SWCNT, two pulse charges, and two charged AFM force probes. Our design can overcome the above-mentioned shortcomings (Problems I and II) of the microfluidic flip-flop designed by us [8]. In particular, the state switch time in our molecular flip-flop reaches the picosecond level, which is about six orders of magnitude faster than that of the microfluidic flip-flop [8]. Moreover, the flip-flop state information can be exported using the charged force probes of AFM.

Experimentally, the size of the flip-flop input/output unit should be estimated. The miniaturization of both AFM probes and nanoelectrodes have been studied for three decades. Nanoelectrodes and AFM probes have been fabricated with radii less than 1 nm [33–38]. For example, carbon nanotubes [33–36] can be used as charged AFM probes owing to their remarkable mechanical and electrical properties. The radius of SWCNTs can be as small as 0.2 nm [34]. If such a probe is connected to a conducting electrode at only one end, charges will be accumulated on the probe surface under the applied potential difference [39]. In this work, we can also choose two 0.2-nm-radius SWCNT probes, which are placed parallel to each other. Provided that the axis-to-axis distance between them is 1.2 nm, the two probes can work independently. In addition, the distance between the probes in experiments may be greater than that utilized in our simulation, and the charge quantities of q_1, q_2, q_A, and q_B should be amplified accordingly. In the area of nanoelectrodes, Penner et al. fabricated a 0.5-nm-radius metallic nanoelectrode in 1990 [37]. Moreover, SWCNTs can also be used as nanoelectrodes [40,41]. Considering that the sizes of the apices of current AFM probes and nanoelectrodes are similar to that of our model framework, experimental demonstrations are promising.

In this work, we design a molecular-level flip-flop using a water molecule and SWCNTs. Our results provide insight into related processes and investigations of other polar-molecule-based flip-flops. Such flip-flops originate from the interaction between polar molecules and nonuniform electric fields. Here, we considered the potential applications for these flip-flops, such as molecular computing. Molecular computing utilizes individual atoms or molecules to solve computational problem. For example, in 1994, Adleman first demonstrated that DNA molecules could be used to solve certain computational problems [42]; in 2004, Benenson et al. realized autonomous molecular computing using DNA and RNA molecules [43]; and Park et al. performed molecular logic-gate operations using biomolecules and metal ions in 2010 [44]. Molecular computing requires basic elements, such as logic gates, memories, and flip-flops. Therefore, our work could be applied to molecular computing.

Y.W. acknowledges the financial support by the National Natural Science Foundation of China under Grant No. 11304284 and by the Research and Development Foundation of ZAFU under Grant Nos. 2012FR064 and 2013FR018. J.P.H. acknowledges the financial support by the National Natural Science Foundation of China under Grant Nos. 11075035 and 11222544, by the Fok Ying Tung Education Foundation under Grant No. 131008, by the Program for New Century Excellent Talents in University (NCET-12-0121), and by the Shanghai Rising-Star Program (No. 12QA1400200). The computational resources utilized in this research were provided by Shanghai Supercomputer Center.

References

1. M.M. Mano, C.R. Kime, *Logic and Computer Design Fundamentals* (Pearsone education international, New Jersey, 2004)
2. T. Thorsen, S.J. Maerkl, S.R. Quake, Science **298**, 580 (2002)
3. M. Prakash, N. Gershenfeld, Science **315**, 832 (2007)
4. M.W. Toepke, V.V. Abhyankar, D.J. Beebe, Lab Chip **7**, 1449 (2007)
5. H. Craighead, Nature **442**, 387 (2006)
6. P. Yager, T. Edwards, E. Fu, K. Helton, K. Nelson, M.R. Tam, B.H. Weigl, Nature **442**, 412 (2006)
7. J. Do, C.H. Ahn, Lab Chip **8**, 542 (2008)
8. X.X. Zhao, Y. Gao, J.P. Huang, J. Appl. Phys. **105**, 064510 (2009)
9. D.D. Kemp, M.S. Gordon, J. Phys. Chem. A **112**, 4885 (2008)
10. G. Hummer, J.C. Rasaiah, J.P. Noworyta, Nature **414**, 188 (2001)
11. K. Akiyama, T. Eguchi, T. An, Y. Fujikawa, Y. Yamada-Takamura, T. Sakurai, Y. Hasegawaa, Rev. Sci. Instrum. **76**, 033705 (2005)
12. A. Agronin, Y. Rosenwaks, G. Rosenman, Appl. Phys. Lett. **85**, 452 (2004)
13. D.H. Kim, J.Y. Koo, J.J. Kim, Eur. Phys. J. Appl. Phys. **28**, 301 (2004)
14. K. Koga, G.T. Gao, H. Tanaka, X.C. Zeng, Nature **412**, 802 (2001)
15. J.Y. Li, X.J. Gong, H.J. Lu, D. Li, H.P. Fang, R.H. Zhou, Proc. Natl. Acad. Sci. USA **104**, 3687 (2007)
16. B. Wang, P. Král, Phys. Rev. Lett. **98**, 266102 (2007)
17. Y.S. Tu, P. Xiu, R.Z. Wan, J. Hu, R.H. Zhou, H.P. Fang, Proc. Natl. Acad. Sci. USA **106**, 18120 (2009)
18. P. Xiu, B. Zhou, W.P. Qi, H.J. Lu, Y.S. Tu, H.P. Fang, J. Am. Chem. Soc. **131**, 2840 (2009)
19. Y. Wang, Y.J. Zhao, J.P. Huang, J. Phys. Chem. B **115**, 13275 (2011)
20. X.W. Meng, Y. Wang, Y.J. Zhao, J.P. Huang, J. Phys. Chem. B **115**, 4768 (2011)
21. K.F. Rinne, S. Gekle, D.J. Bonthuis, R.R. Netz, Nano. Lett. **12**, 1780 (2012)
22. X.W. Meng, J.P. Huang, Phys. Rev. E **88**, 014104 (2013)
23. D. Tasis, N. Tagmatarchis, A. Bianco, M. Prato, Chem. Rev. **106**, 1105 (2006)
24. A. Yaya, C.P. Ewels, Ph. Wagner, I. Suarez-Martinez, A. Gebramariam Tekley, L. Rosgaard Jensen, Eur. Phys. J. Appl. Phys. **54**, 10401 (2011)

25. H. Grubmüller, B. Heymann, P. Tavan, Science **271**, 997 (1996)
26. P.E. Marszalek, H. Lu, H. Li, M. Carrion-Vazquez, A.F. Oberhauser, K. Schulten, J.M. Fernandez, Nature **402**, 100 (1999)
27. Y. Xu, J. Shen, X. Luo, I. Silman, J.L. Sussman, K. Chen, H. Jiang, J. Am. Chem. Soc. **125**, 11340 (2003)
28. Y. Wang, L.X. Zhang, J. Polym. Sci. Polym. Phys. **45**, 2322 (2007)
29. G. Bussi, D. Donadio, M. Parrinello, J. Chem. Phys. **126**, 014101 (2007)
30. B. Hess, C. Kutzner, D. Van De Spoel, E. Lindahl, J. Chem. Theory. Comp. **4**, 435 (2008)
31. P.M. Agrawal, B.M. Rice, D.L. Thompson, Surf. Sci. **515**, 21 (2002)
32. W.L. Jorgensen, J. Chandrasekhar, J.D. Madura, R.W. Impey, M.L. Klein, J. Chem. Phys. **79**, 926 (1983)
33. N.R. Wilson, J.V. Macpherson, Nat. Nanotechnol. **4**, 483 (2009)
34. L. Chen, C.L. Cheung, P.D. Ashby, C.M. Lieber, Nano. Lett. **4**, 1725 (2004)
35. J.H. Hafner, C. Cheung, T.H. Oosterkamp, C.M. Lieber, J. Phys. Chem. B **105**, 743 (2001)
36. C.L. Cheung, J.H. Hafner, C.M. Lieber, Proc. Natl. Acad. Sci. USA **97**, 3809 (2000)
37. R.M. Penner, M.J. Heben, T.L. Longin, N.S. Lewis, Science **250**, 1118 (1990)
38. D.W.M. Arrigan, Analyst **129**, 1157 (2004)
39. C. Li, E.T. Thostenson, T.W. Chou, Compos. Sci. Technol. **68**, 1227 (2008)
40. J.M. Bonard, M. Croci, C. Klinke, R. Kurt, O. Noury, N. Weiss, Carbon **40**, 1715 (2002)
41. I. Heller, J. Kong, H.A. Heering, K.A. Williams, S.G. Lemay, C. Dekker, Nano. Lett. **5**, 137 (2005)
42. L.M. Adleman, Science **266**, 1021 (1994)
43. Y. Benenson, B. Gil, U. Ben-Dor, R. Adar, E. Shapiro, Nature **429**, 423 (2004)
44. K.S. Park, C. Jung, H.G. Park, Angew. Chem. Int. Ed. **49**, 9757 (2010)